Cement & Concrete Composites 40 (2013) 30–39

Contents lists available at SciVerse ScienceDirect

Cement & Concrete Composites

journal homepage: www.elsevier.com/locate/cemconcomp

Degradation kinetics and aging mechanisms on sisal fiber cement composite systems

João de Almeida Melo Filho [a], Flávio de Andrade Silva [b,*], Romildo Dias Toledo Filho [b]

[a] Civil Engineering Department, Universidade Federal do Amazonas, CEP 69077-000 Manaus, AM, Brazil
[b] Civil Engineering Department, COPPE, Universidade Federal do Rio de Janeiro, P.O. Box 68506, CEP 21941-972 Rio de Janeiro, RJ, Brazil

ARTICLE INFO

Article history:
Received 17 September 2012
Received in revised form 6 April 2013
Accepted 8 April 2013
Available online 18 April 2013

Keywords:
Durability
Natural fibers
Cementitious composites

ABSTRACT

The kinetics of vegetable (sisal) fiber degradation and the mechanisms responsible for deterioration of continuous sisal fiber cement composites are presented in this paper. Two matrices were used: one with 50% partial cement replacement by metakaolin (PC–MK) and a reference matrix having as binder only Portland cement (PC). The durability performance of the composite systems is examined and the mechanisms for the significant delay in the fiber degradation when the total amount of calcium hydroxide is reduced from the matrix discussed. The composites were subjected to 5, 10, 15, 20 and 25 cycles of wetting and drying and then tested under a four point bending load configuration in order to determine the flexural behavior and cracking mechanisms with progressive aging. Furthermore, composites stored under controlled lab conditions were tested under bending load at ages ranging from 28 days to 5 years. Fibers extracted from the aged composites were subjected to thermal analysis, Fourier transform infrared spectroscopy and microscopical observations in order to evaluate the changes in chemical composition and microstructure. Two fiber degradation mechanisms were observed in the PC composites: fiber mineralization due to the precipitation of calcium hydroxide in the fiber cell and surface and degradation of cellulose, hemicellulose and lignin due to the adsorption of calcium and hydroxyl ions. The degradation process occurs rapidly and after 10 cycles of wetting/drying a quite expressive modification in the flexural behavior is observed. The residual mechanical parameters after 25 cycles were the same as those observed in the unreinforced matrix. For the PC–MK composite fiber mineralization was not observed due to the low content of CH in the matrix.

1. Introduction

Continuous sisal fiber cement composites are a new class of material which exhibits a multiple cracking behavior with strain hardening under tension and bending loads [1]. This composite system presents an enhanced strength and ductility performance which is primarily governed by the fiber–matrix interface [2] which allows for a fiber bridging and bonding mechanism resulting in the development of a distributed micro-crack pattern. More recent investigations demonstrated the high energy absorption capacity of continuous sisal fiber composites when submitted to impulse loadings [3,4]. This behavior was attributed to the pull-out failure mechanism observed in this composite system. High damage tolerance during tensile fatigue tests was also observed in earlier works [5].

Sisal as well as other natural fiber cement based composites produced with ordinary Portland cement (OPC) matrices undergo an enhanced aging process, while submitted to a humid environment during which they may suffer a reduction in ultimate strength and toughness. The aging process is due to fiber mineralization and results in a reduction of the tensile strength of fibers and a decrease of the fiber pull-out ligament after fracture. This mineralization process is a result of migration of hydration products (mainly $Ca(OH)_2$) to the fiber structure. Several works found in the literature discussed the durability problem of natural fibers when used in a cement based matrix and some of them presented counter-measures to avoid the fiber mineralization process [6–18]. The most promising treatment is the partial substitution of Portland cement by pozzolanic materials in order to reduce the amount of calcium hydroxide in the matrix.

Juarez et al. [11] performed wetting and drying cycles in cement based composites reinforced by the natural fiber Agave lecheguilla (V_f = 1% and L_f = 20–30 mm). The fibers were treated with paraffin and the composite produced with partial cement replacement by fly ash at a dosage of 60% (W/C = 0.65) and 15% (W/C = 0.35) by cement weight. Exposure to 15 cycles of wetting and drying at constant temperature of 70 °C and temperature variations (70 °C for drying and 21 °C for wetting) were performed. Flexural tests performed after the accelerating aging cycles resulted in a decrease

* Corresponding author. Tel.: +55 21 2562 8493x48; fax: +55 21 2562 8484.
E-mail address: fsilva@coc.ufrj.br (Flávio de Andrade Silva).

0958-9465/$ - see front matter © 2013 Elsevier Ltd. All rights reserved.
http://dx.doi.org/10.1016/j.cemconcomp.2013.04.003

Fig. 1. The sisal plant and its fiber: (a) a sisal leaf showing the sisal fiber distribution, (b) the fiber after being extracted and cleaned and (c) the microstructure of the sisal fiber which is formed by several fiber-cells.

in strength from 5.9 MPa to 5.3 MPa (for constant temperature) and to 5.1 MPa (varying the temperature) when the W/C ratio was 0.65.

Toledo and co-workers [9] evaluated sisal and coir fiber reinforced cement composites durability by means of accelerated aging processes. Counter-measures to avoid fiber degradation such as carbonation of the matrix in a CO_2-rich environment, immersion of fibers in slurried silica fume prior to incorporation in the ordinary Portland cement matrix, partial replacement of OPC matrix by undensified silica fume or blast-furnace slag and a combination of fiber immersion in slurried silica fume and cement replacement was investigated. Regarding to the tests in specimens with partial cement replacement by pozzolanic materials the results obtained indicate that the treatment of the matrix with undensified silica fume was an effective means of slowing down the strength loss and embrittlement of the composites. The specimens incorporating slag were quite sensitive to the cycles of wet and dry and presented a strong deterioration with time.

Mohr et al. [17] used several supplementary cementitious materials as partial cement replacement to mitigate kraft pulp fiber (Slash Pine softwoods) cement degradation during accelerate aging cycles. It was proposed that the initial calcium hydroxide content in the composite plays a significant role in minimizing degradation during the wetting and drying cycles. Improvements in the composite durability were most likely related to a reduction in the calcium hydroxide content and the stabilization of the alkali content.

The previous works [13,14] performed by the authors confirmed that the partial cement replacement by pozzolanic materials in order to complete the consumption of the calcium hydroxide produced during the cement hydration process is the most promising treatment resulting in a composite with increased durability. Results have shown that continuous sisal fiber cement-based composites produced with a matrix with low contents of calcium hydroxide preserved its original toughness and strength even when subjected to 100 wetting and drying cycles. However, none of the past works have explained the degradation kinetics of the natural fiber at the various scales of the composite system.

In the present work continuous sisal fiber cement based composites were produced using two matrices: one with 50% partial cement replacement by metakaolin (PC–MK) and the other composed by ordinary Portland cement only (PC). Thermogravimetric analysis was used to investigate the development of the cement hydration products as a function of age. The two developed composites were subjected to laboratory controlled wetting and drying cycles. The composites were subjected to 5, 10, 15, 20 and 25 aging cycles and then tested under a four point bending load configuration. A high resolution digital camera was used to take and record images during the tests at regular intervals. The images were processed in an image analysis program to correlate crack spacing to the applied displacement after being submitted to the various cycles. Furthermore, PC–MK composites were tested under bending load at ages ranging from 28 days to 5 years. A microstructural investigation was performed, using a scanning electron microscope, to observe the degree of degradation in the fibers after being exposed to the cycles. Fibers extracted from the composites were subjected to thermal gravimetric analysis and Fourier transform infrared spectroscopy in order to determine if any of the chemical compounds presented in the sisal fiber were degraded after the accelerated aging process. Finally, the fiber degradation mechanisms were discussed.

2. Materials and methods

2.1. The sisal fiber

The sisal fibers were obtained from the sisal plant (see Fig. 1a) cultivated in farms located in the Bahia state, Brazil. They were extracted from the sisal plant leaves in the form of long fiber bundles (see Fig. 1b–d). The fiber extraction from the leaf was done by semi-automatic raspadors. From a 100 kg of sisal leaves about 3.5 kg extractable fiber is obtained. These fibers were characterized mechanically by Silva et al. [19–21]. Monotonic tension tests were performed in fibers with gage lengths ranging from 10 to 40 mm. The sisal fibers presented mean elastic modulus and tensile strength around 19 GPa and 400 MPa, respectively.

Regarding to the sisal fiber microstructure it is formed by numerous individual fibers (fiber-cells) which are about 6–30 μm in diameter (Fig. 1d). The individual fiber-cells are linked together by means of the middle lamella. The chemical composition of the sisal fiber comprehends approximately 54–66% cellulose, 12–17% hemicellulose, 7–14% lignin, 1% pectin and 1–7% ash. To be used as reinforcement in the developed composite, the sisal fibers were washed in hot water, brushed to separate the individual fibers and cut to the size of the molds (400 mm). The fibers were weighted and separated into five different layers resulting in a total volume fraction of 6%. The sisal fibers were stitched by three cotton fibers to make a homogeneous spacing between the fibers so as to facilitate the molding process.

2.2. Matrix design

Two matrices were designed using the Portland cement CPII F-32 defined by the Brazilian standard [22] as composed with filler (in mass: 85% < clinker < 91%; 3% < gypsum < 5%; 6% < filler < 10%) with a 32 MPa compressive strength at 28 days. The PC matrix which was composed only by Portland cement and the PC–MK matrix which had a partial cement replacement by 50% of amorphous metakaolin. The amount of cement replacement by MK has been defined in the authoŕs previous work [23]. The mortar matrix used in this study presented a mix design of 1:1:0.4 (cementitious

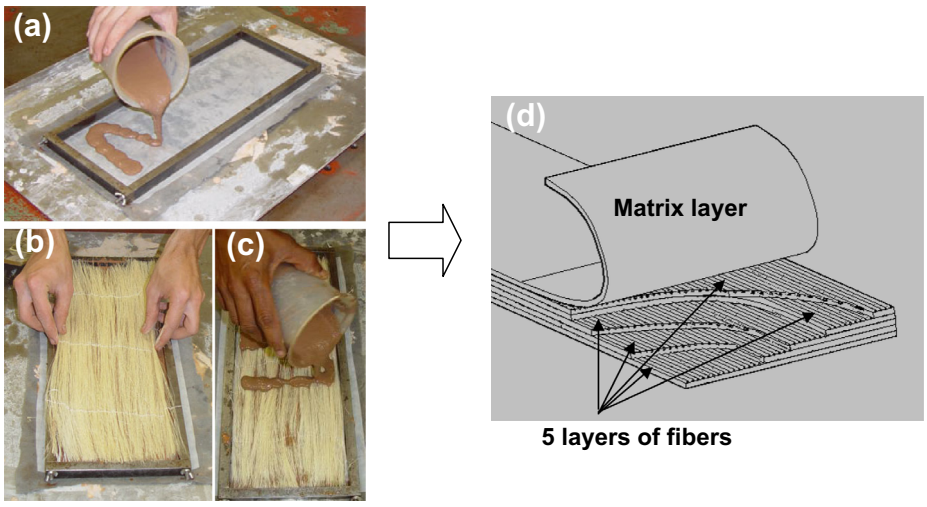

Fig. 2. The composite molding procedure: (a) the first layer of matrix being poured in the mold, (b) placement of the first fiber layer, (c) placement of the second matrix layer and (d) an overview of the composite layers.

material:sand:water by weight). In order to achieve the desired rheology (flow table spread of 400 mm) 2% of superplasticizer was used.

2.3. Composite production

The matrix was produced using a bench-mounted mechanical mixer with a capacity of 20 l. The cementitious materials were dry mixed for 30 s (for homogenization) with the subsequent addition of sand. The powder material was mixed for 30 s more and the superplasticizer previously diluted in the water was slowly poured into the running mixer and subsequently mixed for 3 min. For the production of the laminates, the mortar mix was placed in a steel mold by a manual lay-out technique, one layer at a time, followed by one layer of fibers and vibration (see Fig. 2). The total amount of fibers used as reinforcement were distributed over five layers and represents a volume fraction of 6%. The composites were fog cured for 28 days in a cure chamber with 100% relative humidity (RH) and 23 ± 1 °C.

2.4. Test methods

2.4.1. Mechanical properties

Four point bending tests were performed before and after controlled cycles of wetting and drying and at ages ranging from 28 days to 5 years. For the drying cycles a forced air flow chamber (FAFC) was used. The FAFC was designed in the author's previous work [13] in order to allow the control of the wind velocity and air temperature enabling a simulation of the environmental conditions to which the material can be subjected in practical applications. In the present study the FAFC was set to a temperature of 36 ± 1 °C and wind velocity of 0.5 m/s. The length of the wetting and drying cycles was determined in the author's previous work [13] as one day under water followed by 2 days of drying under the FAFC conditions. For the tests at the various ages the composites were stored in the FAFC at the same conditions as those described above.

The bending tests were carried out at an actuator displacement rate of 0.5 mm/min. Three specimens with geometry of 400 mm × 100 mm × 12 mm (length × width × thickness) were tested under a four point bending configuration (300 mm span) as can be seen in Fig. 3. Displacements at mid-span were measured using electrical transducers (LVDTs) and were continuously recorded, together with the corresponding loads.

The cracking development of the composite was recorded during the loading cycle of the bending test at regular time intervals for posterior image analysis. A Nikon D90 digital camera with an AF Micro Nikkor 60 mm lens ($f/2.8D$) and frame grabber captured images of 4288 × 2848 pixels in resolution at 60 s intervals (see Fig. 3). Images were used to measure the crack spacing during bending tests performed before and after the aging cycles. Photos of the tension face in bending were taken using a mirror positioned at 45° with respect to the specimen as shown in Fig. 3.

2.4.2. Microstructural analysis

The sisal fiber microstructure was investigated before and after exposition to the cycles of wetting and drying. The morphological microstructural investigation was performed using a Jeol JSM 6460 LV scanning electron microscope operating under a low vacuum chamber to remove the high vacuum constraint in the sample environment. Samples subjected to the aging cycles were observed under an accelerating voltage ranging from 10 kV to 20 kV. The specimen chamber pressure was adjusted to values ranging from 25 to 80 Pa. All the micrographs were taken under the backscattered electrons mode.

To investigate the fiber surface an Environmental Scanning Electron Microscope (ESEM) model XL30-ESEM was used. The ESEM was operated under low vacuum. All the micrographs were

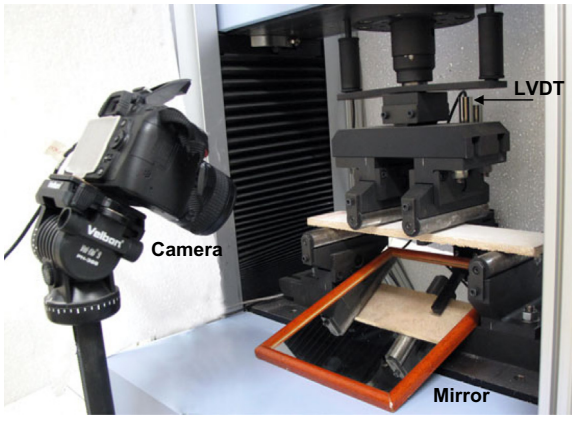

Fig. 3. The four-point bending test set-up. The test was coupled with image analysis to measure the composite cracking spacing as a function of displacement and load.

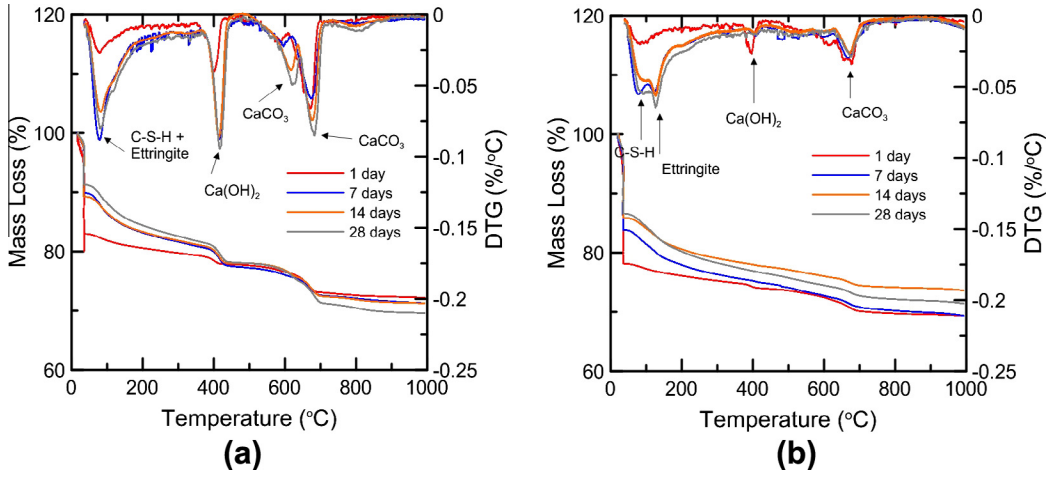

Fig. 4. TG and DTG analysis performed in (a) PC matrix and (b) PC–MK matrix in ages ranging from 1 to 28 days.

taken under the gaseous secondary electron (GSE) detector mode at accelerating voltages of 20 and 30 kV and chamber pressure of 0.6–0.7 mbar.

For both techniques no coating with carbon or gold, as is usually done for high vacuum SEM, was required.

2.4.3. Thermal analysis

Thermal analysis was performed for the developed cement based matrices at 1, 7, 14 and 28 days of curing and in the fibers extracted from the aged composites. The tests were performed in a SDT Q600 simultaneous TGA/DTA/DSC from TA Instruments. The hydrated paste samples were initially dried at 35 °C for 1 h in the equipment before the constant heating rate step of 10 °C/min was initiated from 35 °C to 1000 °C. Samples weighing 10 mg were submitted to the testing conditions in a platinum crucible using 100 ml/min of nitrogen as the purge gas. For the fiber analysis the system was operated at a heating rate of 10 °C/min from 22 °C until 800 °C under the same conditions as described above.

2.4.4. Fourier transform infrared (FTIR) spectroscopy

FTIR analyses were performed with a Bruker Vector 22 FTIR Spectrometer connected with an IRscope II microscope. The sisal fibers which were embedded in the PC and PC–MK matrices were manually selected from the composites before and after exposition to 25 cycles of wetting and drying. The fibers were cooled using liquid nitrogen and then grinded in a pebble mill. The grinded fibers were transformed into tablets (2% w/w of fibers) with KBr. These tablets were then subjected to a pressure of 8 tons/cm^2 for 5 min. The spectra were recorded over the range of 4000 to 500 cm^{-1}, with a resolution of 4 cm^{-1}, and averaged over 32 scans. The spectrometer was operated with diffuse reflection mode at an interaction angle of 45° and a probe area of 0.6 mm diameter; the sampling depth (at 1000 cm^{-1}) was calculated to be approximately 3 μm.

3. Results and discussion

3.1. Evolution of the cement paste microstructure

The results of the thermogravimetric (TG) analysis performed in the PC and PC–MK matrices at ages ranging from 1 to 28 days are shown in Fig. 4. All curves are presented in a cement calcined mass basis in order to have a similar method for comparison and for same composition. This was based on the methodology first established by Dweck and co-workers [24]. In a general manner the results can be better visualized by the peaks of the TG derivative (DTG) which correspond to the several steps of mass loss. It can be seen that between 35 and 200 °C the DTG peak indicate a loss of combined water which comes initially from the calcium silicate hydrate (C–S–H) and then from ettringite. Following, it can be observed the dehydroxylation of the calcium hydroxide (CH) which occurs between 370 and 470 °C and, finally, between 600 and 730 °C, the decomposition of calcium carbonate and other carbonates present in the initial cement composition which occurs due to the loss of CO_2.

It can be observed from Figs. 4 and 5 that the amount of calcium hydroxide gradually increases in the PC matrix from 0.42 g/g (6% of the calcined mass) at 7 days to 0.1 g/g (15% of the calcined mass) up to 28 days. In the opposite way the PC–MK matrix presents a lower formation of calcium hydroxide at 1 day of age followed by a rapid reduction resulting in a matrix with no signs of CH at 28 days of age. This lower initial amount at one day was calculated to be 0.02 g/g (2.78% of the calcined mass).

This mechanism can be explained due to the fact that designing a matrix with a blend of Portland cement and amorphous metakaolin leads to a hydration process where the secondary pozzolanic reaction is causing a lowering of the calcium hydroxide content. Initially, the silicate clinker minerals will react under the formation of calcium silicate hydrates (C–S–H) gel and calcium hydroxide.

$$C_3S + H \rightarrow C{-}S{-}H + CH + \text{heat} \quad (1)$$

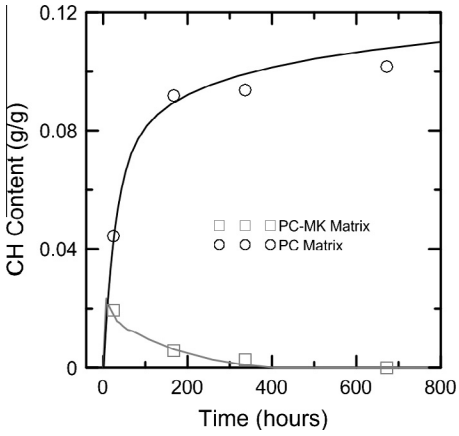

Fig. 5. Evolution of CH content in the PC and PC–MK matrices as a function of time.

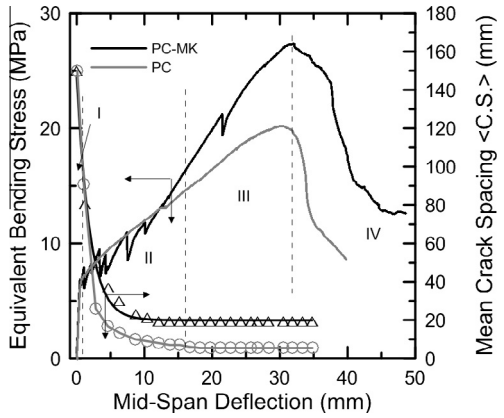

Fig. 6. Flexural and fracture behavior of PC–MK and PC composites performed at 28 days of age.

$$C_2S + H \rightarrow C{-}S{-}H + CH + \text{heat} \quad (2)$$

When the amorphous metakaolin was added to the Portland cement, they reacted with calcium hydroxide forming C–S–H in an exothermic reaction as shown in the following equation:

$$S + CH + H \rightarrow C{-}S{-}H + \text{heat} \quad (3)$$

The secondary pozzolanic reaction will impose an additional transformation of the hydration products. However, as the metakolin contains a significant portion of Al_2O_3, the components dissolving from the metakaolin and water form a secondary C–A–S–H gel that includes the contributions of both pozzolanic and PC hydration reactions. This secondary C–A–S–H gel has a similar structure compared to a C–S–H gel, with a partial replacement of the silicium ions by aluminum ions in the bridging tetrahedral of its structure [25].

3.2. Mechanical tests and microstructural analysis

Fig. 6 shows one representative flexural stress–deflection curve for the PC–MK and PC composites tested at 28 days of age. The results of the evaluation for all curves are given in Table 1. In general it can be seen that both PC–MK and PC composites present a deflection hardening response with a multiple cracking formation. The flexural behavior begins with an elastic-linear range where both matrix and the fiber behave linearly up to a point where the matrix cracks (zone I). The PC–MK composite presented a limit of proportionality (LOP) of 6.67 MPa while for the PC composite a value of 4.95 MPa was reported. Standard deviations varied from 0.45 to 0.74 MPa. The post LOP range was characterized by a multiple cracking formation (zone II) until no more cracks can form. The widening of the existing cracks takes place in region III where the crack spacing becomes constant. The computed crack spacing was 19.25 mm for the PC–MK and 5.44 mm for the PC composite. The failure of the composites occurred after a mid-span deflection of around 27 mm (PC composite) and 31 mm (PC–MK composite). The failure was followed by a strain softening response due to the localization and widening of one of the existing cracks (zone IV). The ultimate flexural strength values observed for the PC and PC–MK composites were 18.73 and 26.86 MPa, respectively.

In the present work the toughness was measured as the area under the load vs. deflection curve up to the ultimate bending strength. The toughness obtained by the PC–MK composite was 22% higher than that of the PC. In the same way as observed in the author's previous work [13] a superior number of cracks with lower width was reported for the PC composites (34 cracks) in comparison to the PC–MK (15 cracks). This behavior may indicate a higher fiber–matrix bond adhesion for the PC composite system.

Fig. 7 shows one representative flexural stress–deflection curve for the PC–MK and PC composites tested under bending load after being exposed to 5, 10, 15, 20 and 25 cycles of wetting and drying. The results of the evaluation for all curves are given in Table 1. It can be observed that the LOP increased with the aging process in the two studied systems (refer to Table 1). This can be explained by the fact that more hydration products were formed as a result of the accelerated aging which leaded to an increase in the matrix strength. For the PC–MK system a ductile behavior with a multiple cracking formation is observed not only for the reference specimens but also for the aged ones. On the other hand the PC composites presented a progressive degradation process with the cycles. It can be seen that both the ductility and bending strength reduced to the same level of an unreinforced matrix after 25 cycles of wetting and drying.

From Fig. 8 it can be seen that the accelerated aging process is more severe in the first 10 cycles for the PC composite. The PC systems toughness lowered from 13.94 to 3.67 kJ/m^2 at 10 cycles and further decreased to 0.07 kJ/m^2 after 25 cycles. The reduction in the bending strength reached the same value (7.4 MPa) of the unreinforced matrix after 25 cycles. From these results we can first conclude that 10 cycles is a threshold level where most of the degradation in the fiber and fiber–matrix interface takes place and that the sisal fiber completely degrades when the PC composite is aged at 25 cycles.

For the PC–MK composite the toughness values decreased from 17.09 to 10.31 kJ/m^2. The bending strength presented a reduction in the first 10 cycles from 28.86 MPa to 21.64 MPa. After 10 cycles of aging the variation in the mean bending strength values were not statistically representative. As no degradation was observed in the sisal fibers extracted from the composite, no reduction in

Table 1
Results of four point bending tests of PC–MK and PC composites before and after exposition to the accelerated aging cycles (mean ± standard deviation).

Mix	Aging time (Cycles)	LOP (MPa)	Displacement at LOP (mm)	Flexural strength (MPa)	Displacement at flexural strength (mm)	Toughness (kJ/m^2)	Number of cracks	Mean final crack spacing (mm)
PC–MK	0	6.67 (0.74)	0.51 (0.073)	26.86 (0.75)	26.15 (1.36)	17.09 (1.53)	15.0 (2.1)	19.25 (4.94)
	5	8.57 (0.29)	0.55 (0.015)	24.95 (1.58)	26.13 (1.85)	13.70 (0.99)	14.0 (1.0)	15.54 (7.00)
	10	8.11 (1.24)	0.54 (0.085)	21.64 (0.89)	25.64 (1.57)	14.18 (1.27)	11.0 (1.0)	20.00 (3.00)
	15	7.64 (1.23)	0.53 (0.064)	22.63 (0.46)	27.14 (0.74)	12.39 (1.49)	11.0 (0.6)	19.00 (3.00)
	20	7.78 (0.24)	0.51 (0.093)	21.24 (0.32)	24.90 (0.81)	11.80 (1.48)	12.0 (3.1)	18.40 (3.10)
	25	7.90 (0.28)	0.53 (0.055)	20.58 (0.16)	25.07 (0.25)	10.31 (0.32)	11.0 (1.2)	17.24 (5.80)
PC	0	4.95 (0.45)	0.46 (0.015)	18.73 (1.36)	27.49 (0.74)	13.94 (2.75)	34.0 (2.1)	5.44 (2.12)
	5	6.55 (0.79)	0.47 (0.066)	15.87 (0.03)	20.89 (0.09)	7.83 (0.27)	16.0 (2.0)	9.00 (2.90)
	10	6.39 (0.73)	0.49 (0.065)	10.98 (0.86)	13.57 (0.70)	3.67 (0.88)	15.0 (1.5)	12.52 (6.18)
	15	6.90 (0.21)	0.44 (0.053)	9.07 (0.86)	8.50 (1.11)	1.68 (0.30)	7.0 (1.0)	21.00 (11.92)
	20	6.85 (0.77)	0.47 (0.038)	6.85 (0.39)	0.47 (0.04)	0.36 (0.07)	1.0 (0.6)	91.00 (2.00)
	25	6.93 (0.42)	0.49 (0.065)	6.93 (0.42)	0.49 (0.06)	0.07 (0.007)	1.0 (0.0)	91.00 (2.36)

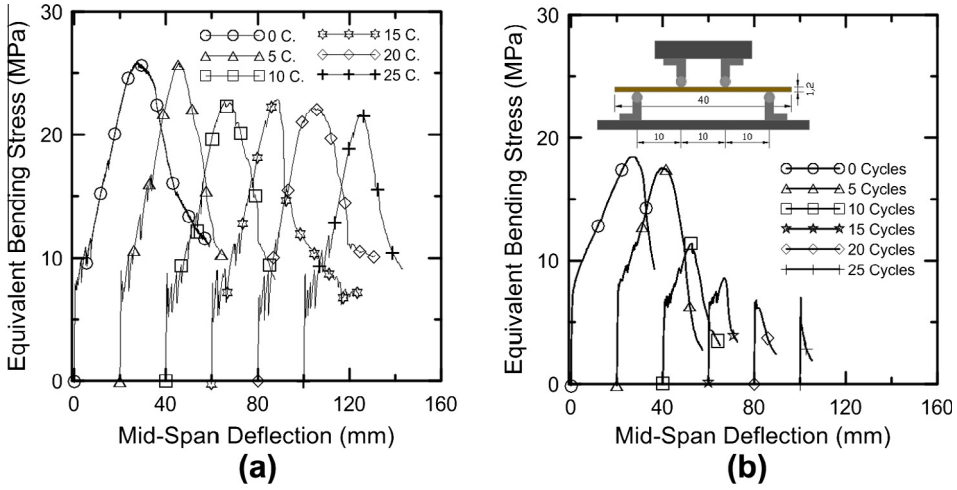

Fig. 7. Effect of the wetting and drying cycles on the mechanical behavior under bending load of (a) PC–MK composite and (b) PC composite.

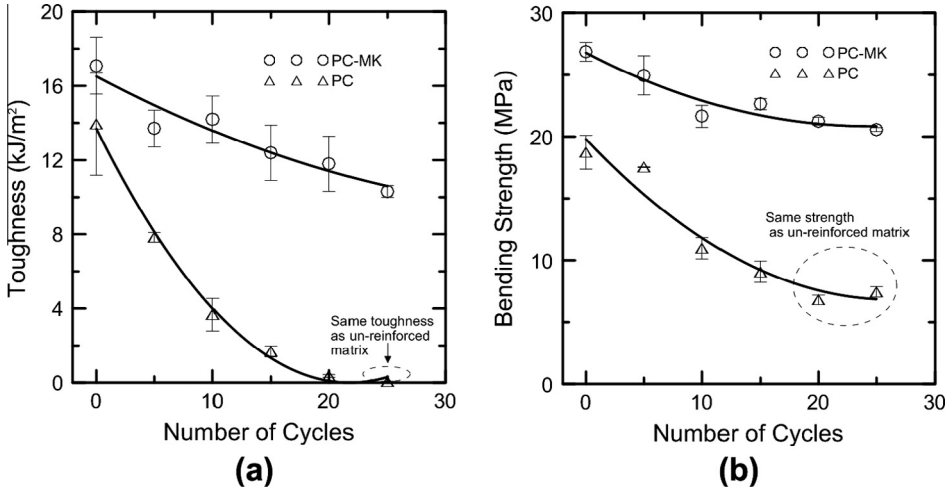

Fig. 8. Effect of the wetting and drying cycles on the (a) toughness and (b) bending strength of PC–MK and PC composites.

the stiffness of the post-cracking region was observed and no changes in the cracking pattern occurred, the authors explain the decrease in bending strength and ductility as follow. In the first 10 cycles there was a change in the fiber–matrix interfacial shear mechanisms. The frictional stress may have lowered after the first 10 cycles as a result of an interface fatigue mechanism. This is due to the volumetric variation of the sisal fibers as a result of the wetting and drying cycles. After 10 cycles the fibers undergo a hornification process [26] which is characterized by the stiffening of the polymeric structure presented in the fiber cell wall as a result of the water removal. This process reduces the fiber volumetric variation mitigating the damage in the fiber–matrix interface. Further studies are necessary to confirm the author's hypothesis.

The effect of the aging cycles in the crack spacing is presented in Fig. 9. The aging process seems not to affect the fracture behavior of the PC–MK composite. Its crack spacing is around 19 mm with a standard deviation that ranges from 3 to 7 mm. In a different manner the cycles are affecting the fracture process of the PC composite and changing its behavior from a multiple to a single cracking formation. Again it seems that there is a threshold level around 10 cycles for the PC composite. After this point the number of cracks drastically reduces from 34 to 15 and then to one (after 20 cycles).

Fig. 10 presents the typical curves of four-point bending tests performed in PC–MK composites from 28 days to 5 years. Table 2

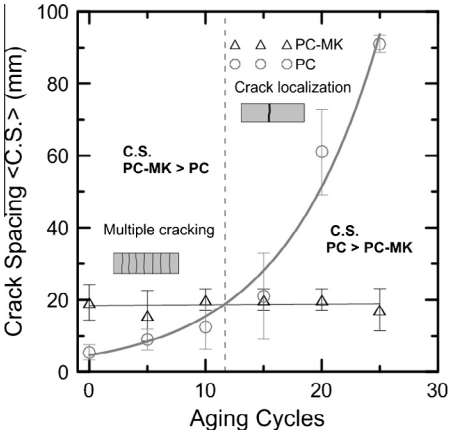

Fig. 9. Effect of wetting and drying cycles on the crack spacing of PC–MK and PC composites.

reports the mean values and standard deviation for all test conditions. It can be seen that the LOP increases from 9.66 to 11.33 MPa and the bending strength did not present any representative alteration. From Fig. 10b it is noticed an increase in the post-cracking

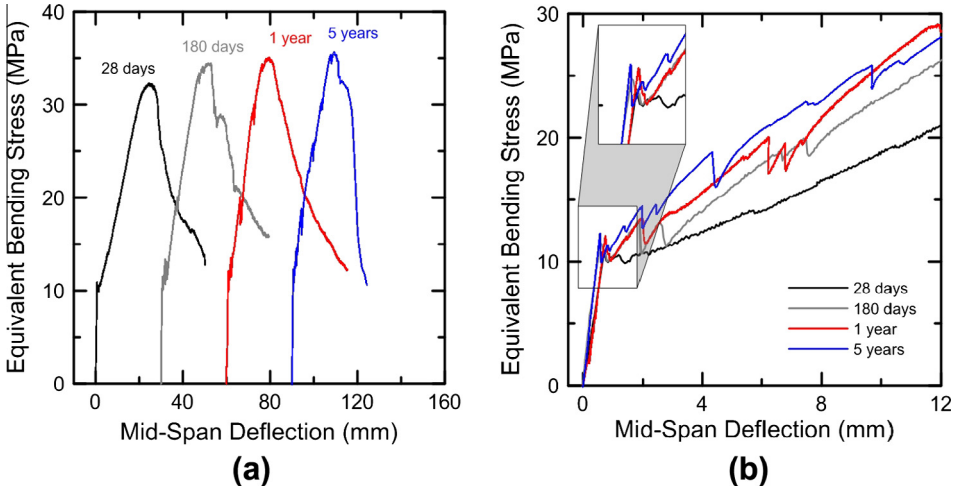

Fig. 10. Effect of natural aging on (a) the ultimate flexural strength and (b) on the postcracking stiffness of PC–MK composites subjected to flexural loading.

Table 2
Results of four point bending tests performed in PC–MK composites subjected to natural aging (mean ± standard deviation).

Natural aging time	LOP (MPa)	Displacement at LOP (mm)	Flexural strength (MPa)	Displacement at flexural strength (mm)	Toughness (kJ/m^2)	Number of cracks	Mean final crack spacing (mm)
28 days	9.66 (0.33)	0.65 (0.09)	32.50 (0.62)	24.77 (0.04)	20.77 (1.03)	17.0	12.0 (2.0)
180 days	10.55 (1.17)	0.59 (0.06)	34.89 (0.78)	22.49 (0.90)	21.43 (0.91)	7.5	18.0 (1.3)
1 year	10.41 (1.46)	0.54 (0.13)	34.07 (1.33)	19.75 (0.46)	17.88 (1.98)	5.0	19.0 (2.2)
5 years	11.33 (1.00)	0.46 (0.01)	33.36 (2.02)	16.70 (1.73)	17.87 (2.30)	5.0	19.0 (2.2)

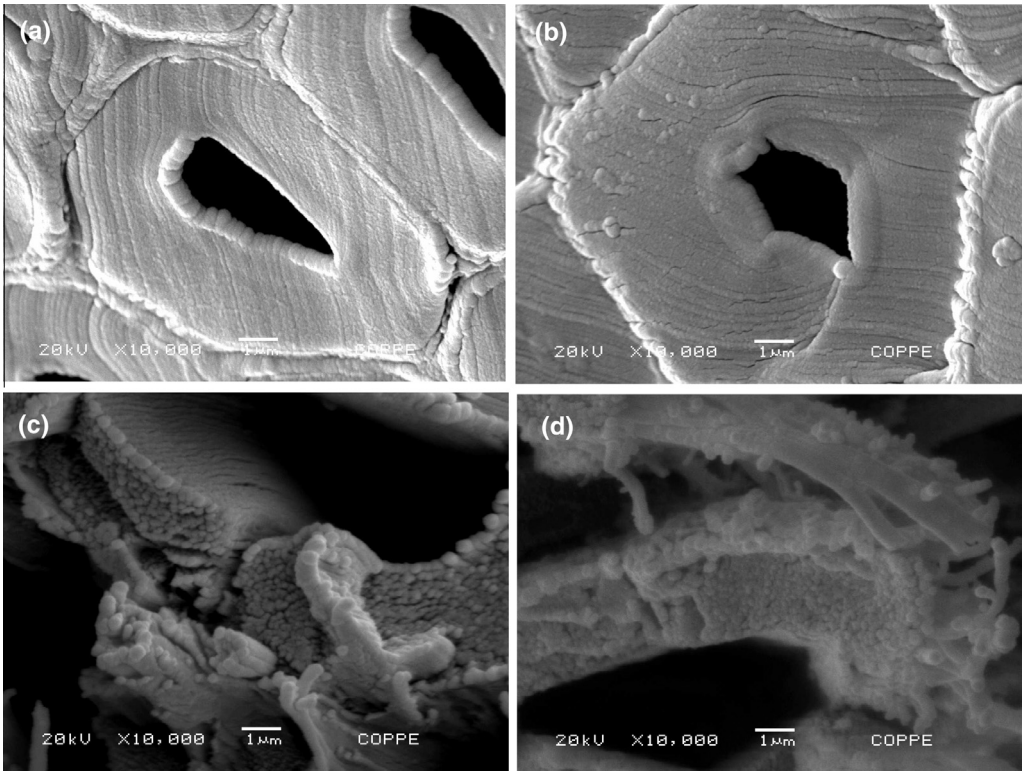

Fig. 11. The effect of the wetting and drying cycles on the sisal fiber microstructure: (a) reference, (b) fiber extracted from a PC–MK matrix after 25 cycles, (c and d) fiber extracted from a PC matrix after 25 cycles.

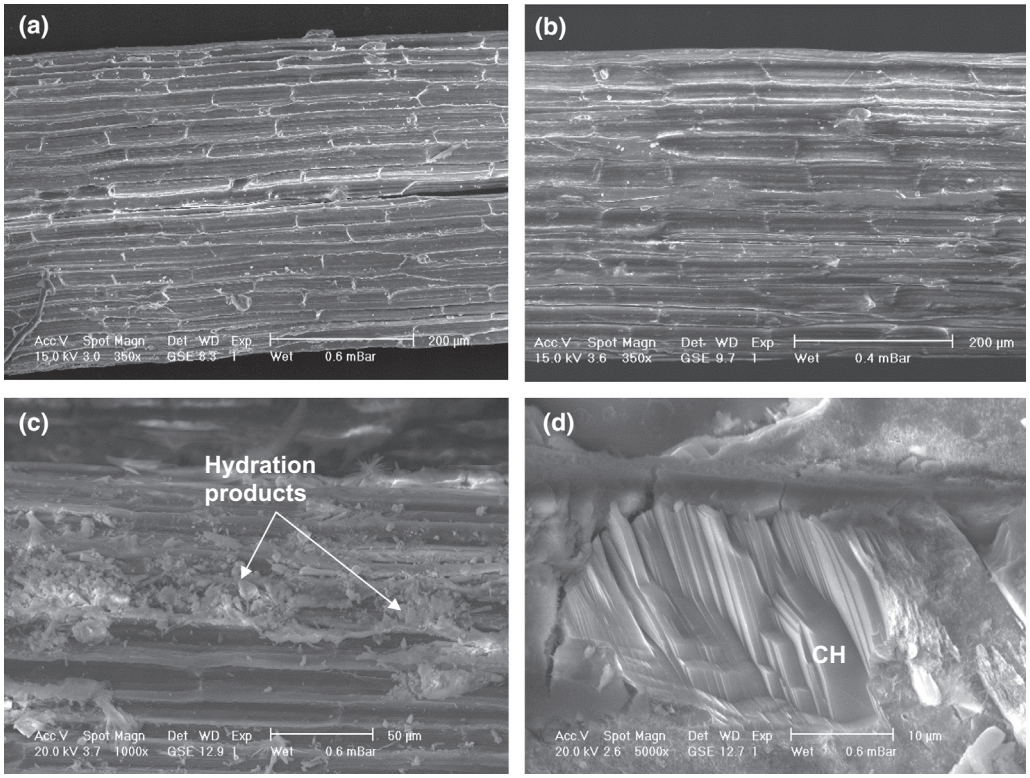

Fig. 12. The effect of the wetting and drying cycles on the sisal fiber surface: (a) reference, (b) fiber extracted from a PC–MK matrix after 25 cycles, (c and d) fiber extracted from a PC matrix after 25 cycles.

region (zone II) as a function of age which results in a reduction of the composite ductility. The stiffness increased from 1.71 to 2.37 GPa for ages of 28 days and 5 years. A reduction in the number of cracks from 17 (at 28 days) to 5 (at 5 years) was reported. This behavior can be traced back to a change in the elastic bond component of the system. During debonding, the shear stress intensity in the elastically bonded region may increase with age as a result of fiber–matrix densification. The frictional bond strength is not being altered with age as the bending strength is remaining constant.

A microstructural investigation was performed in the fibers extracted from the PC–MK and PC aged composites to investigate their degradation process. Fig. 11 shows SEM micrographs of fibers in natura (reference) and after being exposed to 25 cycles of wetting and drying. As for comparison purposes all the micrographs show one single fiber cell obtained using the same magnification and the same working distance. In Fig. 11b it can be seem that the fiber structure of the sisal extracted from the PC–MK composite remains intact with no signs of degradation. In Fig. 11c and d it is presented the sisal fiber micro-structure after being exposed to 25 cycles inside the PC composite. The sisal micro-structure shows clear signs of degradation indicating that part of the material that composes the fiber cell wall was degenerated. This micro-structure analysis confirms that in the PC composite the fiber-cells are mineralized possibly due to the high calcium hydroxide concentration.

Fig. 12 shows the micrographs of the sisal fibers surface in natura and after exposition to 25 cycles in the two studied matrices. No signs of calcium hydroxide were found in the fiber surface extracted from the PC–MK composites. The fiber surface showed in Fig. 12b, which was extracted from the PC–MK matrix, is a representative sample which accurately reflects those of the larger group of investigated fibers. On the fiber's surface extracted from the PC matrix it was observed a high concentration of hydration products (Fig. 12c) including calcium hydroxide crystals which is presented in Fig. 12d.

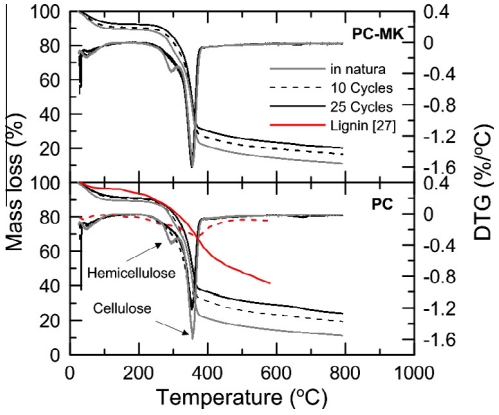

Fig. 13. TG and DTG analysis on the fibers extracted from the PC–MK and PC composites. The lignin curve was obtained from Ref. [27].

The addition of metakaolin has successfully sustained the capacity of energy absorption of the PC–MK composite, increasing its first crack strength and maintaining its ultimate strength through accelerated aging, proving to be a good solution for the durability issues of natural fiber reinforced cement based composites.

3.3. Sisal fiber degradation process

Fig. 13 shows the curves of thermogravimetric (TG) and differential thermogravimetric (DTG) analysis performed on natural sisal fibers and extracted from the aged composites. The DTG curve of the natural sisal fibers shows a weight loss of 7.6% in the temperature range of 31–171 °C, which is due to the loss of adsorbed water in the fiber (refer to Table 3). The DTG curves reveal a strong shoulder peak at the left side of the main peak for the

Table 3
Results of the TG analysis performed in the sisal fiber before and after exposition to the aging cycles.

Samples	Initial weight loss		Active pyrolysis		Char region	
	Temperature (°C)	Wt. loss (%)	Temperature (°C)	Wt. loss (%)	Temperature (°C)	Wt. loss (%)
In natura	31.0–171	7.6	172–450	72.6	450–792	8.6
10 Cycles PC	31.2–171	9.9	172–450	61.77	450–792	7.3
25 Cycles PC	31.8–171	9.8	172–450	56.73	450–792	9.4
10 Cycles PC–MK	31.2–171	7.1	172–450	68.59	450–792	7.0
25 Cycles PC–MK	31.3–171	9.6	172–450	62.85	450–792	7.3

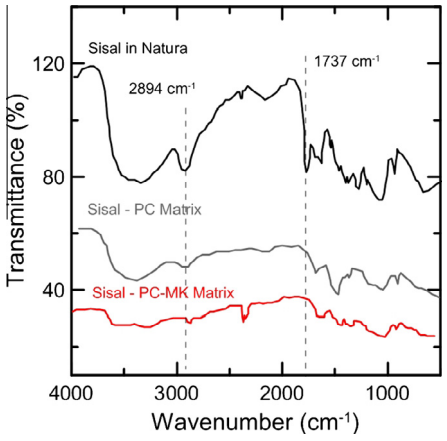

Fig. 14. FTIR spectra for natural sisal fiber and after exposition to 25 cycles of wetting and drying in the PC–MK and PC composites.

natural sisal fibers. This shoulder peak is attributed to the hemicellulose present in the fiber while the main peak corresponds to the degradation of cellulose as indicated in Fig. 13. The hemicellulose was found to decompose at the temperature of 290 °C. The thermal decomposition of cellulose begins to occur at 210 °C by dehydration followed by major endothermic reaction of depolymerization with DTG peaks at 360 °C. Lignin is known to degrade over a wide range which usually starts at 173 °C with DTG peaks at 367 °C and it cannot be seen in the sisal fiber TGA [27]. To illustrate the lignin decomposition and peaks a curve obtained from the literature [27] was included in Fig. 13.

The hemicellulose peak was not observed for the fibers extracted from both matrices after the aging process. A reduction in the peak of cellulose is observed from fibers extracted from both matrices after 25 cycles but to a greater extent for the fiber extracted from the PC composite. In the fibers extracted from the PC matrix it was observed a 15% weight loss in the peak of cellulose while in the PC–MK matrix a loss of 5% was noticed. As lignin decomposition peak is very close to that of cellulose and cannot be located when performing a TG analysis in sisal fibers it must not be affirmed that the decomposition peak refers only to cellulose. Furthermore, cellulose is a polymer made of repeating glucose molecules attached end to end which is very difficult to dissolve due to the extensive network of hydrogen bonds and van der Waals interaction forces between the cellulose fibrils. Therefore the authors explain the weight loss around 360 °C as follows. The fibers aged in the PC matrix presented a combined degradation of lignin and cellulose while the fibers in the PC–MK system presented only lignin deterioration.

Fig. 14 presents the FTIR spectra for the natural sisal fiber and after exposition to 25 cycles of wetting and drying in the PC–MK and PC matrices. The natural sisal shows a distinct wave at about 1737 cm^{-1}. This stands for the carboxyl-group and is present in the structure of lignin. The sisal fiber presents a number of bands in the 1650–1750 regions related to the presence of aldehyde, keto, carboxyl and ester groups which are present in the lignin and hemicellulose structures. The absorption peak intensities at about 2893 cm^{-1} indicates the CH_2/CH_3 wave stands for the hemicellulose. It is visible from Fig. 14 that the bands related to lignin and hemicellulose is obviously decomposed in both of the matrices after the aging process.

The authors suggest two mechanisms for the sisal fiber degradation which is illustrated in Fig. 15. The main mechanism is the deposition of calcium hydroxide crystals at the fiber surface which has been observed in the SEM micrographs presented in Fig. 11. The deposition of calcium hydroxide in the fiber surface leads to

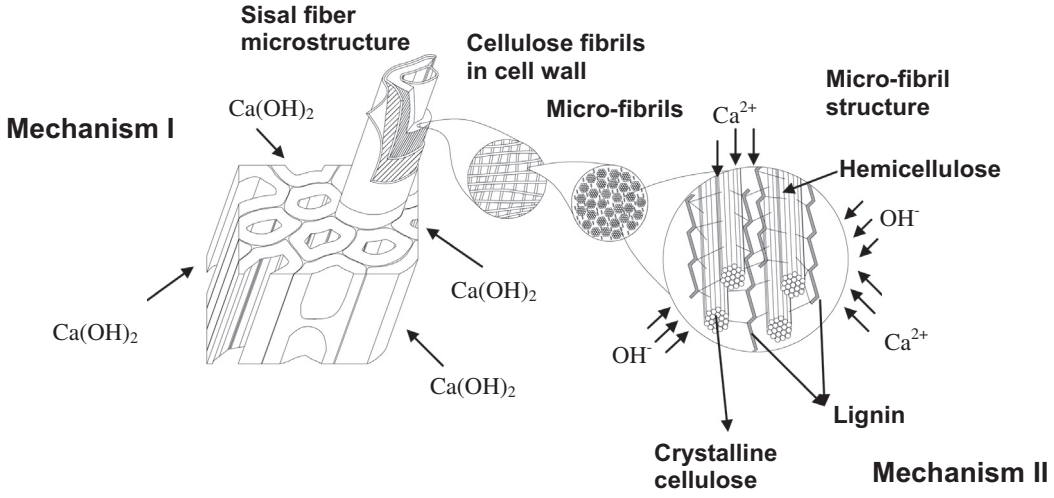

Fig. 15. Sisal fiber degradation mechanisms in a Portland cement environment.

a fiber mineralization process. This may also reduce the amount of cellulose in the fiber as suggested by the TG analysis. In this process the fibeŕs ductility and strength decreases which has been confirmed by the mechanical tests presented in Fig. 7.

A secondary and less severe mechanism is the hemicellulose and lignin degradation. Both TGA and FTIR techniques showed a decomposition of hemicellulose and lignin in sisal fibers presented in the two studied matrices after the cycles of wetting and drying. The author's hypothesis is the adsorption of calcium and hydroxyl ions by the sisal fiber surface. According to [28] the NaOH and $Ca(OH)_2$ treatments leads to the removal of amorphous materials from the fiber surface like waxes, fats, hemicelluloses and lignin. As lignin and hemicellulose are responsible for linking the microfibril structure their degradation may also lead to a reduction in the macro mechanical properties of the sisal fiber.

4. Conclusions

The following conclusions can be drawn from the present work on the durability mechanisms of sisal fiber cement based composites:

- The thermogravimetric analysis indicated that the Portland cement replacement by 50% of amorphous metakaolin lead to a significant reduce of the calcium hydroxide formation. It was not detected any sign of calcium hydroxide at 28 days by using the methodologies described in the present work.
- Flexural tests performed after the accelerated aging cycles showed that the PC composite system completely loses its ductility and strength after 25 cycles of wetting and drying. It was observed that the accelerated aging process is more severe in the first 10 cycles for the PC composite. The residual mechanical parameters after 25 cycles were the same as those observed in un-reinforced matrices. The fracture process changed from a multiple cracking to a single cracking formation after 20 cycles.
- For PC–MK systems the mechanical performance was slight affected by the aging cycles. The cracking pattern has not been altered during the aging cycles and the crack spacing remained constant to around 19 mm. A small reduction in strength and toughness were noticed during the first 10 cycles. The authors related this phenomenon to a fatigue in the fiber matrix-interface due to the volumetric changes of the sisal fiber with the wetting and drying cycles.
- PC–MK composites tested after curing ages ranging from 28 days to 5 years showed a progressive increase in the post-cracking stiffness resulting in a decrease of toughness and cracking density.
- Microstructural observation suggested that the sisal fibers undergo a mineralization process when used as reinforcement in conventional Portland cement matrices. The cell walls of the fibers were damage after the wetting and drying cycles. No signs of fiber degradation were noticed for sisal fibers exposed to the aging process in PC–MK composites.
- Thermogravimetric analysis performed in the sisal fiber revealed that both lignin and hemicellulose are degraded when the fiber is exposed, in both matrices, to the cycles. For the PC matrix it was observed a 15% weight loss in the peak of cellulose while in the PC–MK matrix a loss of 5% was noticed. The authoŕs hypothesis is that cellulose is also being degraded in fibers used for reinforcing the PC matrix.
- FTIR showed that lignin and hemicellulose degrades in sisal fibers extracted from PC and PC–MK matrices after aging exposition. This confirmed the results obtained from the TG analysis.
- The authors suggest two mechanisms for the sisal fiber degradation: the main mechanism – (i) fiber mineralization by calcium hydroxide precipitation in the fiber surface and a secondary and less severe process – (ii) lignin and hemicellulose deterioration through the adsorption of calcium and hydroxyl ions.

References

[1] Silva FA, Mobasher B, Toledo Filho RD. Cracking mechanisms in durable sisal reinforced cement composites. Cem Concr Compos 2009;31:721–30.
[2] Silva FA, Mobasher B, Soranakom C, Toledo Filho RD. Effect of fiber shape and morphology on interfacial bond and cracking behaviors of sisal fiber cement based composites. Cem Concr Compos 2011;33:814–23.
[3] Silva FA, Zhu D, Mobasher B, Soranakom C, Toledo Filho RD. High speed tensile behavior of sisal fiber cement composites. Mater Sci Eng A 2010;527:544–52.
[4] Silva FA, Zhu D, Mobasher B, Toledo Filho RD. Impact behavior of sisal fiber cement composites under flexural load. ACI Mater J 2011;108:168–77.
[5] Silva FA, Mobasher B, Toledo Filho RD. Fatigue behavior of sisal fiber reinforced cement composites. Mater Sci Eng A 2010;527:5507–13.
[6] Gram HE, Person H, Skarendahl A. Natural fibre concrete. SAREC-Report, Swedish Agency for Research Cooperation with Developing Countries, Stockholm; 1984.
[7] Gram HE. Durability of natural fibers in concrete, Swedish Cement and Concrete Research Institute, Research Fo; 1983.
[8] Toledo Filho RD, Scrivener K, England GL, Ghavami K. Durability of alkali-sensitive sisal and coconut fibers in cement mortar composites. Cem Concr Compos 2000;22:127–43.
[9] Toledo Filho RD, Ghavami K, England GL, Scrivener K. Development of vegetable fiber-mortar composites of improved durability. Cem Concr Compos 2003;25:185–96.
[10] Tonoli GHD, Joaquim AP, Arsène MA, Bilba K, Savastano Jr H. Performance and durability of cement based composites reinforced with refined sisal pulp. Mater Manufact Process 2007;22:149–56.
[11] Juárez C, Durán A, Valdez P, Fajardo G. Performance of "*Agave lecheguilla*" natural fiber in Portland cement composites exposed to severe environment conditions. Build Environ 2007;42(3):1151–7.
[12] Mohr BJ, Nanko H, Kurtis KE. Durability of kraft pulp fiber–cement composites to wet/dry cycling. Cem Concr Compos 2005;27(4):435–48.
[13] Toledo Filho RD, Silva FA, Fairbairn EMR, Melo Filho JA. Durability of compression molded sisal fiber reinforced mortar laminates. Constr Build Mater 2009;23:2409–20.
[14] Silva FA, Toledo Filho RD, Melo Filho JA, Fairbairn EMR. Physical and mechanical properties of durable sisal fiber cement composites. Constr Build Mater 2010;24:777–85.
[15] Sera EE, Robles-Austriaco L, Pama RP. Natural fibers as reinforcement. J Ferrocement 1990;20(2):109–24.
[16] Aziz MA, Paramasivam P, Lee SL. Prospects for natural fibre reinforced concretes in construction. Int J Cem Compos Lightweight Concr 1981;3(2):123–32.
[17] Mohr BJ, Biernacki JJ, Kurtis KE. Supplementary cementitious materials for mitigating degradation of kraft pulp fiber–cement composites. Cem Concr Res 2007;37:1531–43.
[18] MacVicar R, Matuana LM, Balatinecz JJ. Aging mechanisms in cellulose fiber reinforced cement composites. Cem Concr Compos 1999;21:189–96.
[19] Silva FA, Chawla N, Toledo Filho RD. Tensile behavior of high performance natural (sisal) fibers. Compos Sci Technol 2008;68:3438–43.
[20] Silva FA, Chawla N, Toledo Filho RD. Mechanical behavior of natural sisal fibers. J Biobased Mater Bioenergy 2010;4:106–13.
[21] Silva FA, Chawla N, Toledo Filho RD. An experimental investigation of the fatigue behavior of sisal fibers. Mater Sci Eng A 2009;516:90–5.
[22] NBR 11578. Cimento Portland Composto. Associação Brasileira de Normas Técnicas (ABNT), Julho; 1991. [in Portuguese].
[23] Melo Filho JA. Chemical and thermal durability and mechanical behavior of high performance sisal cement based composites. Doctoral thesis, Civil Engineering Department, COPPE/UFRJ; 2012. [in Portuguese].
[24] Dweck J, Cunha ALC, Pinto CA, Gonçalves JP, Büchler PM. Thermogravimetry on calcined mass basis – hydrated cement phases and pozzolanic activity quantitative analysis. J Therm Anal Calorim 2009;97:85–9.
[25] Wang S, Scrivener KL. Si-29 and Al-27 NMR study of alkali-activated slag. Cem Concr Res 2003;33:769–74.
[26] Ferreira SR, Lima PRL, Silva FA, Toledo Filho RD. Effect of sisal fiber hornification on the adhesion with Portland cement matrices. Revista Matéria 2012;17:1024–34.
[27] Martin AR, Martins MA, Silva ORRF, Mattoso LHC. Studies on the thermal properties of sisal fiber and its constituents. Thermochim Acta 2010;506:14–9.
[28] Sedan D, Pagnoux C, Chotard T, Smith A, Lejolly D, Gloaguen V, et al. Effect of calcium rich and alkaline solutions on the chemical behaviour of hemp fibres. J Mater Sci 2007;42:9336–42.